Research paper

Long-term impact of *Ophiostoma novo-ulmi* on leaf traits and transpiration of branches in the Dutch elm hybrid 'Dodoens'

Roman Plichta[1,4], Josef Urban[1], Roman Gebauer[1], Miloň Dvořák[2] and Jaroslav Ďurkovič[3]

[1]Department of Forest Botany, Dendrology and Geobiocoenology, Mendel University in Brno, Zemědělská 3, 61300 Brno, Czech Republic; [2]Department of Forest Protection and Wildlife Management, Mendel University in Brno, Zemědělská 3, 61300 Brno, Czech Republic; [3]Department of Phytology, Technical University in Zvolen, T. G. Masaryka 24, 960 53 Zvolen, Slovak Republic; [4]Corresponding author (roman.plichta@mendelu.cz)

To better understand the long-term impact of *Ophiostoma novo-ulmi* Brasier on leaf physiology in 'Dodoens', a Dutch elm disease-tolerant hybrid, measurements of leaf area, leaf dry mass, petiole anatomy, petiole hydraulic conductivity, leaf and branch water potential, and branch sap flow were performed 3 years following an initial artificial inoculation. Although fungal hyphae were detected in fully expanded leaves, neither anatomical nor morphological traits were affected, indicating that there was no impact from the fungal hyphae on the leaves during leaf expansion. In contrast, however, infected trees showed both a lower transpiration rate of branches and a lower sap flow density. The long-term persistence of fungal hyphae inside vessels decreased the xylem hydraulic conductivity, but stomatal regulation of transpiration appeared to be unaffected as the leaf water potential in both infected and non-infected trees was similarly driven by the transpirational demands. Regardless of the fungal infection, leaves with a higher leaf mass per area ratio tended to have a higher leaf area-specific conductivity. Smaller leaves had an increased number of conduits with smaller diameters and thicker cell walls. Such a pattern could increase tolerance towards hydraulic dysfunction. Measurements of water potential and theoretical xylem conductivity revealed that petiole anatomy could predict the maximal transpiration rate. Three years following fungal inoculation, phenotypic expressions for the majority of the examined traits revealed a constitutive nature for their possible role in Dutch elm disease tolerance of 'Dodoens' trees.

Keywords: anatomy, Huber value, LMA, petiole, potential transpiration, sap flow, water potential gradient.

Introduction

Ophiostoma novo-ulmi Brasier is a highly pathogenic fungus causing Dutch elm disease (DED), which has devastated most European elm populations during the current pandemic (Brasier 2000). Dutch elm cultivars of the 1960s and 1970s have shown varying degrees of resistance to DED, and several European elm-breeding programmes have subsequently been established to identify tolerant cultivars such as 'Dodoens' (Ghelardini and Santini 2009). 'Dodoens' tolerance to DED has also been demonstrated in recent studies. Three years following an artificial fungal inoculation by a highly pathogenic strain of *O. novo-ulmi* subsp. *novo-ulmi* × *O. novo-ulmi* subsp. *americana*, no visible symptoms of DED were observed (Ďurkovič et al. 2013). Surprisingly, observations related to the above study using scanning electron microscopy (SEM) revealed that, 3 years after inoculation, fungal hyphae were spreading through functional leaf xylem tissue. The impact of these hyphae on the overall functioning of the infected tree is unknown.

Infection by *Ophiostoma* is characterized by the production of cell wall degrading enzymes (Svaldi and Elgersma 1982, Binz and Canevascini 1996) and high molecular weight toxins (Van Alfen and Turner 1975, Takai and Richards 1978), followed by the formation of alveolar structures, tyloses and gels inside the infected vessels, leading to their occlusion and subsequent cavitation (Newbanks et al. 1983, Ouellette et al. 2004). Thus, it could be assumed that the presence of *Ophiostoma* hyphae inside vessels of 'Dodoens' trees is followed by the dysfunction

of these infected vessels, which are never again used to conduct water. These vessels could decrease xylem hydraulic conductivity to the extent that it leads to leaf water stress (Urban and Dvořák 2014). Infected leaves of 'Dodoens' should respond to such an impediment by lowering the water potential, causing possible additional cavitation and enhanced leaf water stress, and/or by lowering transpiration through stomatal closure and thereby affecting the tree's carbon gain (Larcher 2003, Dias et al. 2014).

Leaf regulation of water vapour loss is required to maintain leaf water potentials above the critical threshold of xylem cavitation and the turgor loss point (Sperry et al. 1998, Guyot et al. 2012). Plants improve leaf water potential regulation when they are exposed to long-lasting water stress and are able to decrease the minimum leaf water potential without deterioration (Otieno et al. 2005). Nevertheless, *Ophiostoma* toxins could also alter water potential regulation, as greater concentrations of toxins could reduce xylem hydraulic conductivity and decrease water potentials below the turgor loss point (Van Alfen and Turner 1975). Based on this possibility, it would be worthwhile to compare transpiration rates of healthy and stressed trees, as sap flow is driven by hydraulic conductivity (closely related to conduit diameter) and water potential gradients. Theoretically, the transpiration rate could be similar in healthy and stressed trees, as lower hydraulic conductivity would be balanced by greater water potential gradients.

Re-infestation of newly developed xylem tissues could lead to chronic stress and to xylem modifications. Leaf water stress is usually accompanied by an increase in leaf mass per area ratio (LMA) or sapwood to leaf area ratio ('Huber value', HV), as leaves that develop with low water availability are denser and have lower expansion rates (Mencuccini and Grace 1995, McDowell et al. 2002, Poorter et al. 2009, Limousin et al. 2010). Leaf density modifications are also accompanied by changes in the xylem structure, as plants form xylem with an increased resistance to drought-induced cavitation in order to withstand lower water potentials (Tyree and Zimmermann 2002, Bréda et al. 2006).

In the present study, 3 years following fungal inoculation, we studied the petiole anatomy, leaf morphological traits (such as LMA and HV), water potential, potential transpiration and maximal measured transpiration rates of branches on infected trees of 'Dodoens'. We hypothesized that the long-term persistence of fungal hyphae inside vessels of infected trees (i) will affect the diameter of petiole vessels and will increase LMA and HV as a consequence of the possible long-term (several years) water stress of leaves and (ii) the transpiration rates of infected and non-infected trees will not differ, as lower hydraulic conductivity will be balanced by greater water potential gradients.

Materials and methods

Study site

The experimental field plot was located at Banská Belá, Slovakia (48°28′N, 18°57′E, 589 m above sea level (a.s.l.)). According to the meteorological station at Arboretum Kysihýbel in Banská Štiavnica (540 m a.s.l.), located 3.6 km southwest of the study site, the climate of the area is characterized by a mean annual temperature of 7.7 °C and a mean annual precipitation of 831 mm. The soil has a silt-loam texture and is classified as Eutric Cambisol formed from the slope deposits of volcanic rocks (andesite and pyroclastic materials).

Plant material, fungal inoculation and host responses

The experiments were conducted on leaves and branches of clonally micropropagated 10-year-old trees of the Dutch elm hybrid cultivar 'Dodoens' (open pollinated *Ulmus glabra* Huds. 'Exoniensis' × *Ulmus wallichiana* Planch. P39) during the 2011 growing season, i.e., 3 years following fungal inoculation. A total of three branches (one branch from each of three trees) without the inoculation treatment and a total of four branches (one branch from each of four trees) inoculated with the fungus were chosen. The height of the trees was 720 ± 61 cm and the stem diameter at breast height was 8.4 ± 1.7 cm. All branches were south oriented, fully exposed to sun, at least 1 m long and with a maximal base diameter of 2 cm. The planting scheme and the distribution of inoculated and control trees are shown in Figure S1 available as Supplementary Data at *Tree Physiology* Online.

A description of tree inoculation was given by Solla et al. (2005) and Ďurkovič et al. (2013). Briefly, the spore suspension (1×10^7 spores ml^{-1}) of *O. novo-ulmi* subsp. *novo-ulmi* × *O. novo-ulmi* subsp. *americana* isolate M3 was inoculated into the current-year annual ring, 20 cm above the base of the stem, at the beginning of June 2008. This isolate proved to be ssp. *americana* in a fertility test and had a cerato-ulmin (*cu*) gene profile of ssp. *americana*, but also had a colony type (*col1*) gene profile of ssp. *novo-ulmi* (Konrad et al. 2002, Dvořák et al. 2007). Fifteen weeks after tree inoculations, expressions of DED symptoms (leaf wilting, yellowing or dying) in infected trees reached up to 10%, but no signs of DED external symptoms were found 3 years later in 2011. Upon fungal infection, distinct discolorations of the stem infection zones were concentrated mostly in the earlywood of the 2008 annual ring (Figure 1a), where they represented 2% of the 2008 annual ring area at a height of 80 cm above the inoculation point. Within both the 2008 and 2009 annual rings, infected trees responded to fungal infection with the formation of barrier zones and an altered pattern of secondary xylem annual ring organization (Figure 1b) compared with that found in non-infected trees (Figure 1c). Fungal hyphae (Figure 1d) were microscopically detected inside vessels of these two annual rings causing a degradation of medium-molecular weight macromolecules of cellulose (Ďurkovič et al. 2014). Within the 2011 annual ring, no discoloration of the wood and no fungal colonizations were observed in the infected trees. However, we occasionally observed minute fungal hyphae inside vessel elements of the leaf midrib primary xylem (Figure 1e).
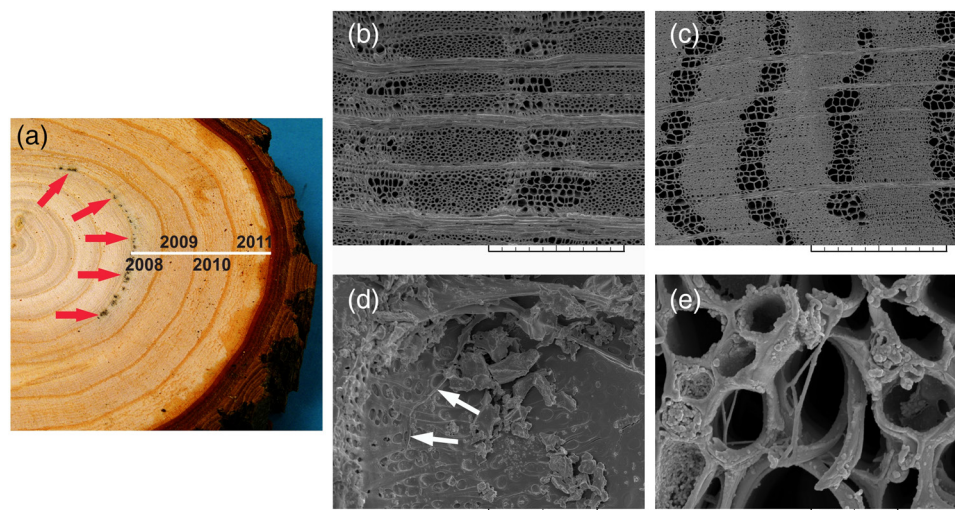
Figure 1. Distribution of DED inside the xylem tissues of infected 'Dodoens' trees. (a) Wood disc cross section, 80 cm above the point of inoculation, showing distinct infection zones (red arrows) concentrated mostly in earlywood of the 2008 annual ring. (b) Formation of many narrowed latewood vessels in the 2009 annual ring in response to fungal infection; SEM, cross section, scale bar = 500 µm. (c) Wild-type pattern of latewood organization in the 2009 annual ring of non-infected trees; SEM, cross section, scale bar = 500 µm. (d) *Ophiostoma novo-ulmi* subsp. *novo-ulmi* × *O. novo-ulmi* subsp. *americana* hyphae (white arrows) inside an earlywood vessel of the 2009 annual ring; SEM, radial section, scale bar = 50 µm. (e) Fungal hyphae inside vessel elements of the leaf midrib primary xylem; SEM, cross section, scale bar = 10 µm. Image (a) is adapted from Ďurkovič et al. (2015); images (d) and (e) are adapted from Ďurkovič et al. (2013).

Scanning electron microscopy images of wood and leaf midrib

In July 2011, fully expanded leaves were sampled from the branches adjacent to those on which sap flow measurements were performed. Leaf midrib (0.4 × 0.4 cm) cross sections were immersed in 5% glutaraldehyde in a 0.1 M cacodylate buffer at pH 7.0, dehydrated in ethanol and acetone, and dried in liquid CO_2 using a Leica EM CPD030 critical point drier (Leica Microsystems, Wetzlar, Germany). After the current-year growing season was completed in November 2011, 4-cm-thick wood discs were sawn from the trunks at a height of 1 m. Both leaf midrib and wood cross sections were mounted on specimen stubs, sputter-coated with gold and observed by high-vacuum SEM using a VEGA TS 5130 instrument (Tescan, Brno, Czech Republic) operating at 15 kV. In all, 18 leaf midrib cross sections and 18 wood cross sections were examined for the presence of fungal hyphae inside xylem conduits of infected trees.

Sap flow and meteorology

Sap flow and meteorology measurements were performed on 26 August 2011. This day was chosen because it was cloudless and followed a period of rain that reduced the likelihood of soil-derived drought stress. Sap flow measurements were performed at the base of the individual branches using the EMS 62 modular sap flow system (EMS, Brno, Czech Republic). Sap flow was measured at 1-min intervals and stored as 10-min averages. In addition, the following meteorological variables were measured near the experimental field plot, using Minikin RTH (EMS) at 1-min intervals and stored as 10-min averages: air temperature at a height of 2 m, air humidity and global radiation. Reference evapotranspiration (ET_0) for the hypothetical grass reference crop was then calculated as described in Allen et al. (1998).

Water potential

Water potentials of leaves (Ψ_l) and branches (Ψ_b) were measured on branches adjacent to the one where the sap flow was measured, using a Scholander pressure chamber PMS 1000 (PMS Instrument Co., Albany, OR, USA). To determine Ψ_b, one branch per tree was enclosed in a black plastic bag to prevent transpiration. The water potential of the enclosed leaves was then measured, based on the assumption that the water potential of the enclosed leaves equilibrated to the water potential in the branches (Riceter 1973, Bauerle et al. 1999). The measurements were performed on 26 August 2011 at 2-h intervals from 06:00 to 18:00 hours.

Leaf and branch traits

Branches were cut at the point of sap flow measurement. Then, branch length (l_b) and branch basal xylem area without pith (A_{xb}) were measured using a tape measure and an Olympus SZX7 zoom stereo microscope (Olympus Czech Group Corporation, Prague, Czech Republic), respectively. Maximal sap flow density at the branch base (Q_{max}) was calculated by dividing the maximal measured sap flow rate by A_{xb}. All leaves from individual branches were arranged from the smallest to the largest, and each sixth or seventh leaf (based on total number of leaves) was chosen for detailed analysis. For each branch, 8–32 sample leaves were collected. Sample leaves were scanned and the leaf area without petioles was measured using image analysis ImageJ

1.45 software. Sample leaves were then oven-dried at 60 °C for 48 h and weighed. Mean leaf area (A_l) was calculated from the sample leaves, and total leaf area (A_b) plus total leaf dry mass (m_b) per branch were then recalculated based on the number of sample leaves and the total number of leaves per branch (n). The trait LMA was calculated as the ratio of leaf dry mass to leaf area, and the HV and HV_m were calculated as the ratios of A_{xb} to A_b and m_b, respectively.

Petiole anatomy

Twenty petioles per branch were sampled. Petioles were fixed in FAA solution (90 ml of 70% ethanol, 5 ml acetic acid and 5 ml of 40% formaldehyde). Cross sections were taken manually with a razor blade from petioles slightly above the pulvilus, and were stained with phloroglucinol and HCl to highlight cell wall lignification by red staining. Stained sections were examined using an Olympus BX51 light microscope (Olympus Czech Group Corporation) and photographed with an Olympus E-330 digital camera (Olympus Czech Group Corporation) using QuickPHOTO Micro 2.3 software (Promicra, Prague, Czech Republic). On the micrographs obtained, all vessel lumens were manually coloured using Adobe Photoshop 9.0.2 software (Adobe Systems Inc., San Jose, CA, USA). For each cross section, the maximal diameter (d_{max}), minimal diameter (d_{min}) and lumen area (A_{lum}) of each vessel were measured within the petiole xylem area (A_{xl}) using ImageJ 1.45 software. Mean diameter of vessels responsible for 95% of hydraulic conductivity (D_{95}) was determined as described by Tyree and Zimmermann (2002). Vessel lumen area percentage (N_A) and vessel density (N_n) were calculated per unit area of A_{xl}.

Measured transpiration and potential transpiration of branches

Leaf area-specific transpiration rate (E) was calculated by dividing the measured sap flow rate by A_b. Accordingly, the maximal E (E_{max}) was calculated from maximal sap flow rate. Theoretical hydraulic conductivity was used to infer potential transpiration rate. The theoretical hydraulic conductivity of each vessel (k_{vess}) was calculated according to the Hagen–Poiseuille law (Cruiziat et al. 2002, Woodruff et al. 2008) (Eq. (1)). Because the cross section of the vessel lumen was fitted by an ellipse, a modification to the formula was applied as recommended by Martre et al. (2000) and Nobel (2005) (Eq. (2)). The theoretical hydraulic conductivity of the petiole cross section (k_p) was calculated as the sum of all k_{vess} in the petiole. Then, the leaf area-specific potential transpiration rate (E_{th}) was derived from the theoretical mass flow through the petioles (Eq. (3)).

$$k_{vess} = \left(\frac{\pi \rho}{8\eta} \right) r_{lum}^4 \tag{1}$$

$$r_{lum}^4 = \frac{d_{max}^3 d_{min}^3}{8 d_{max}^2 + 8 d_{min}^2} \tag{2}$$

$$E_{th} = \frac{\bar{k}_p n \Delta \Psi}{l_b A_b} \tag{3}$$

where ρ is the density of water at 20 °C (998.205 kg m^{-3}), η is the viscosity of water at 20 °C (1.002×10^{-9} MPa s), r_{lum} is the lumen radius, n is the total number of leaves and $\Delta \Psi$ is the maximal difference between leaf and branch water potentials ($\Psi_l - \Psi_b$).

Xylem area-specific conductivity (k_x), leaf area-specific conductivity (k_l) and leaf mass-specific conductivity (k_m) were then calculated as k_p divided by xylem area (A_{xl}), leaf area (A_b) and leaf mass (m_b), respectively.

Abbreviations of the traits used in this study are given in Table 1.

Statistical analysis

Data were analysed using multiple analysis of variance, which was complemented by analysis of variance for each dependent variable. Differences between infected and non-infected trees were evaluated using the Student's t-test, with the significance limit set to $P < 0.05$. Multivariate associations were analysed with a principal component analysis (PCA) to describe patterns of covariation among leaf, branch and ecophysiological traits. Mean values are presented with ± standard deviation (SD). Statistical analysis was carried out using the R statistical program (R Development Core Team 2012).

Table 1. Overview of the traits studied, their abbreviations and the units used throughout this study.

Trait	Explanation	Unit
A_b	Branch leaf area	m^2
A_l	Leaf area	cm^2
A_{xb}	Branch basal xylem area	mm^2
A_{xl}	Leaf petiole xylem area	mm^2
D_{95}	95th percentile vessel diameter	μm
E	Measured transpiration	g m^{-2} h^{-1}
E_{max}	Maximal measured transpiration	g m^{-2} h^{-1}
E_{th}	Theoretical transpiration	g m^{-2} h^{-1}
ET_0	Reference evapotranspiration	g m^{-2} h^{-1}
HV	Huber value per leaf area	m^2 m^{-2}
HV_m	Huber value per leaf dry mass	mm^2 g^{-1}
k_l	Leaf area-specific hydraulic conductivity	kg m^{-1} MPa^{-1} s^{-1}
k_m	Leaf dry mass-specific hydraulic conductivity	kg kg^{-1} m MPa^{-1} s^{-1}
k_x	Petiole xylem area-specific hydraulic conductivity	kg m^{-1} MPa^{-1} s^{-1}
l_b	Branch length	m
LMA	Leaf mass per area ratio	g m^{-2}
m_b	Leaf dry mass	g
n	Number of leaves	–
N_A	Vessel lumen area percentage	%
N_n	Vessel elements density	no. per mm^2
Q_{max}	Maximal sap flow density	g mm^{-2} h^{-1}
Ψ_l	Leaf water potential	MPa
Ψ_{min}	Minimal leaf water potential	MPa
$\Delta \Psi$	Gradient of water potential	MPa m^{-1}

Results

Influence of the fungus on transpiration of branches and the examined traits

The mean predawn water potential was -0.3 ± 0.14 MPa irrespective of fungal infection, indicating adequate soil water availability. The ET_0 reached a maximum of 800 g m^{-2} h^{-1}. The transpiration rate (E) of infected trees was found to be lower from morning until late afternoon than that of non-infected trees (Figure 2). Accordingly, maximum branch transpiration rates (E_{max}) were 42% lower in infected versus non-infected trees ($P = 0.036$, Table 2), while the calculated potential transpiration rate (E_{th}, Eq. (3)) showed no difference between the two treatments. Even though E_{max} of infected trees was lower, no significant differences were observed between infected and non-infected trees in the daily course of leaf water potential (Ψ_l, Figure 3), minimum leaf water potential (Ψ_{min}) and gradient of water potential ($\Delta\Psi$, Table 2). Infected trees had also a lower maximal sap flow density (Q_{max}, $P = 0.047$, Table 2), which was consistent with a lower E_{max} per unit of branch xylem area (A_{xb}, $P = 0.047$, Table 2) in infected trees. The mean E_{max} of all branches was 191 ± 66 g m^{-2} h^{-1} and was 18% lower than the mean E_{th}. The value of E_{max} in infected trees was on average lower by 20% than E_{th}, in contrast to non-infected trees, where E_{max} exceeded E_{th} by 1%. However, the E_{th} to E_{max} ratio did not differ between infected and non-infected trees ($P = 0.30$, Figure 4). The LMA, HV and HV$_m$ also did not differ between infected and non-infected trees (see Table S1 available as Supplementary Data at *Tree Physiology* Online). Additionally, the A_{xb}, branch leaf area (A_b), leaf dry mass (m_b) and other leaf and branch traits did not differ between these two treatments (see Tables S1 and S2 available as Supplementary Data at *Tree Physiology* Online).

Table 2. Comparison of transpiration, sap flow density and water potential measurements between infected and non-infected trees. Abbreviations are given in Table 1. Data represent means ± SD. Significance is denoted as *$P < 0.05$.

Trait	Unit	Non-infected	Infected	P-value
E_{max}	g m^{-2} h^{-1}	250.38 ± 66.58	145.75 ± 30.23	0.036*
E_{th}	g m^{-2} h^{-1}	250.27 ± 76.44	221.54 ± 116.40	0.728
E_{max} to A_{xb}	–	3.73 ± 0.81	1.66 ± 0.17	0.047*
Q_{max}	g mm^{-2} h^{-1}	1.27 ± 0.49	0.54 ± 0.24	0.047*
Ψ_{min}	MPa	-1.57 ± 0.06	-1.54 ± 0.10	0.359
$\Delta\Psi$	MPa m^{-1}	0.67 ± 0.15	0.58 ± 0.10	0.682
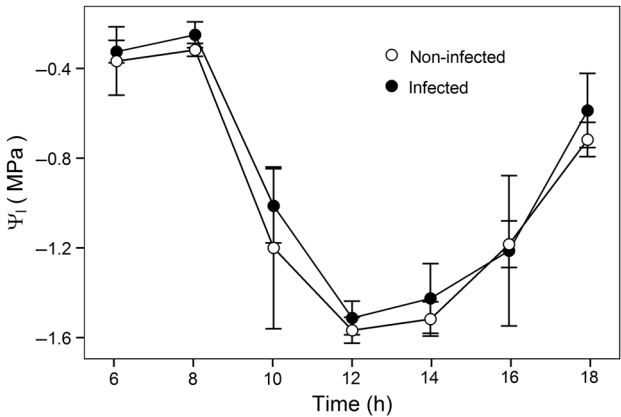
Figure 3. Leaf water potential in infected and non-infected trees from 06:00 to 18:00 hours during the day of measurement (26 August 2011). There is no difference in leaf water potential between infected and non-infected trees. Circles denote mean values and bars denote SD. Abbreviations are given in Table 1.
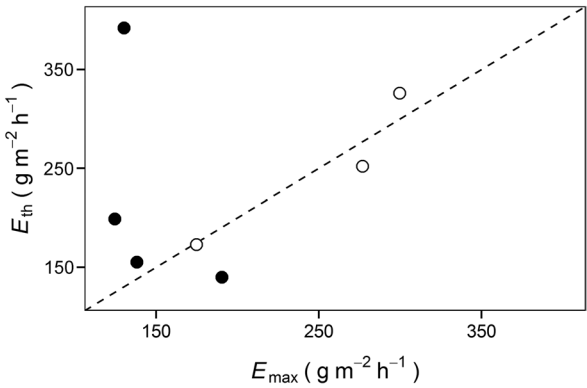
Figure 4. Comparison between the maximal measured transpiration (E_{max}) and calculated potential transpiration (E_{th}). Open circles denote non-infected trees, and closed circles denote infected trees. Dashed line signifies 1 : 1 ratio.

Allometric relationships among the examined traits

The trait E_{th} was positively correlated with LMA ($P = 0.014$, $r^2 = 0.73$, Figure 5) and leaf area-specific hydraulic conductivity (k_l, $P = 0.006$, $r^2 = 0.81$). The LMA was also positively correlated with k_l ($P = 0.03$, $r^2 = 0.64$, Figure 5). Correlation between LMA and petiole xylem area-specific hydraulic conductivity (k_x)
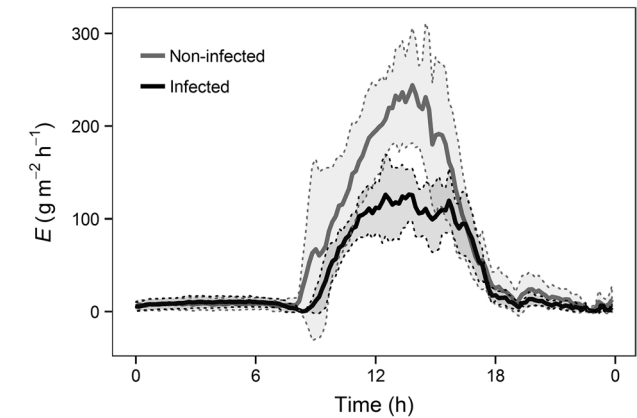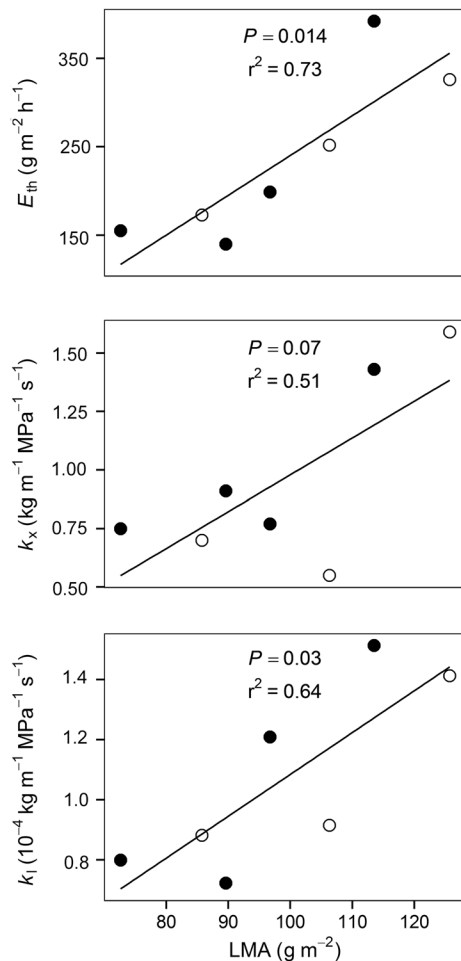

Figure 2. Transpiration of infected and non-infected trees during the day of measurement (26 August 2011). Infected trees show a lower transpiration from the morning until late afternoon. Thick lines indicate average transpiration and grey background with dashed lines indicates SD. Abbreviations are given in Table 1.

Figure 5. Linear dependencies of potential transpiration (E_{th}), xylem area-specific conductivity (k_x) and leaf area-specific conductivity (k_l) on LMA. Open circles denote non-infected trees, and filled circles denote infected trees.

was non-significant ($P = 0.07$, $r^2 = 0.51$, Figure 5), and no relationships have been found between LMA and other leaf traits. However, k_x showed a strong correlation with leaf area (A_l, $P = 0.005$, $r^2 = 0.81$), leaf xylem area (A_{xl}, $P < 0.001$, $r^2 = 0.92$), vessel element density (N_n, $P = 0.005$, $r^2 = 0.82$), vessel lumen area percentage (N_A, $P < 0.001$, $r^2 = 0.98$) and mean vessel diameter (D_{95}, $P < 0.001$, $r^2 = 0.97$, Figure 6). Correlations of this kind, except that between k_x and A_l, could be expected, as hydraulic conductivity is tightly driven by vessel dimensions. The leaf dry mass-specific hydraulic conductivity (k_m) did not show any correlation with other leaf traits except N_n ($P = 0.05$, $r^2 = 0.57$). The trait N_n also correlated with k_l ($P = 0.007$, $r^2 = 0.79$). In addition, neither HV nor HV_m had any significant correlation with any leaf and branch traits other than those used for calculation of HV or HV_m (i.e., A_{xb}, m_b and A_b).

Associations among the examined traits

The first axis of PCA explained 31% of the variation and showed strong negative loadings for LMA, A_l and A_{xl}, and hydraulic traits

such as k_x, k_l and E_{th} (Figure 7, Table S3 available as Supplementary Data at *Tree Physiology* Online). In contrast, a strong positive loading was found for N_n. The second axis explained 21% of the variation and showed strong positive loadings for HV, HV_m and A_{xb}, and a strong negative loading for A_b. The traits E_{max} and $\Delta\Psi$ had a very close association, indicating a strong correlation. Similarly, LMA was closely associated with petiole hydraulic traits (D_{95}, k_x and N_A) as well E_{th}, which connects the petiole hydraulics with $\Delta\Psi$. The multivariate analysis of PCA did not show any distinctive segregation between infected and non-infected trees (Figure 7).

Discussion

Influence of the fungal infection on leaf traits and transpiration of branches

Following rapid earlywood formation in the host during the spring season, the subsequent colonization of earlywood vessels by fungal hyphae may influence both the development of leaf biomass and anatomy as a consequence of the xylem water pathway disturbance (Van Alfen and Turner 1975, Newbanks et al. 1983). The leaves in DED-affected trees frequently show responses similar to those of leaves subjected to drought stress—i.e., LMA and HV increased (McDowell et al. 2002, Poorter et al. 2009, Limousin et al. 2010), and conduit size, leaf area and transpiration rates decreased (Tyree and Zimmermann 2002, Otieno et al. 2005, Bréda et al. 2006, Urban and Dvořák 2014). In infected trees of 'Dodoens', the spreading of fungal hyphae was restricted to the 2008 and 2009 secondary xylem annual rings (Ďurkovič et al. 2014), thereby leaving the current-year annual ring without distinct fungal colonization. This might be a reason why we did not find any significant differences for the majority of the examined leaf and branch traits between infected and non-infected trees. The occasional occurrence of minute fungal hyphae inside vessel elements of the leaf midrib primary xylem might result either from the still continuing sporulation of the hyphae present in vessels of the previous 2008 and 2009 secondary xylem annual rings or from reintroduction of the fungus into the examined branches from the surrounding forest environment. Nevertheless, this event had no direct influence on the anatomical and morphological traits of infected trees during leaf expansion. From a biochemical point of view, such a pattern could be explained by the intrinsic mechanisms of tolerance of the xylem tissues. The host tree cell wall defence system has great ability to impede the spreading of the *Ophiostoma* pathogen (Ouellette and Rioux 1992, Martín et al. 2007, Ďurkovič et al. 2014) by playing a key role in the production of fungitoxic substances (Duchesne 1993, Smalley and Guries 1993, Hubbes 2004).

In contrast to the leaf traits examined in this study, as well as leaf transpiration that was investigated in a previous study by Ďurkovič et al. (2013), infected trees showed a lower transpiration
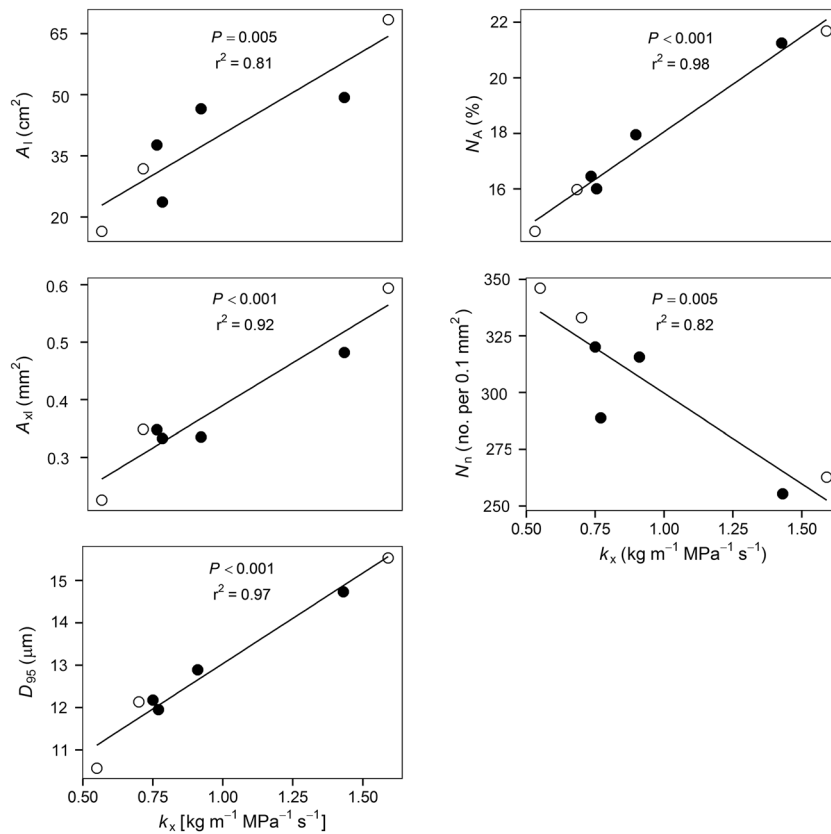
Figure 6. Linear dependencies of leaf area (A_l), petiole xylem area (A_{xl}), mean diameter of vessels (D_{95}), vessel lumen area percentage (N_A) and vessel density (N_n) on xylem area-specific hydraulic conductivity (k_x). Open circles denote non-infected trees, and filled circles denote infected trees.
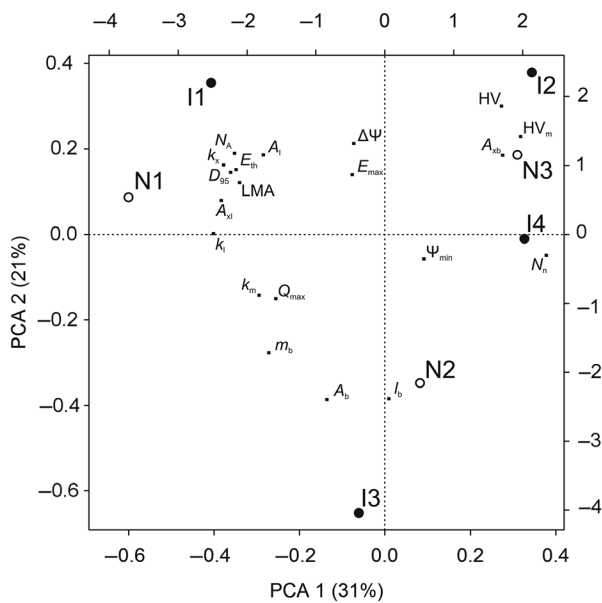

Figure 7. Positions of the examined branch and leaf traits plus positions of the examined trees on the first and second axes of the PCA. The bottom and left-hand axes refer to the examined traits; the top and right-hand axes refer to the examined trees. Percentages of variation explained by each of the axes are given in parentheses. I1–I4 denote infected trees; N1–N3 denote non-infected trees. Trait abbreviations are given in Table 1.

(E) during the day as well as a significantly lower maximal transpiration rate (E_{max}) of branches than non-infected trees. Infected trees also showed a lower sap flow density (Q_{max}) at the base of the branches. We assume that infected trees likely had an increased number of cavitated vessels in either the leaves or the earlywood of branches. Unlike the study of Ďurkovič et al. (2013) where the authors measured leaf transpiration using an infra-red gas analyser equipped with a small leaf cuvette at the end of June 2011, in this study, we measured sap flow within entire branches late in the growing season, at the end of August 2011. Peak evapotranspiration typically occurs during July. We hypothesize that during the growing season, the fungal spores and hyphae spread and grew slowly through the conductive pathways up to the leaf midribs, while the fungal hyphae were producing high molecular weight toxins (Takai and Richards 1978). These toxins are able to decrease the hydraulic conductivity by the occlusion of pit membranes (Van Alfen and Turner 1975), leading to both a blockage and the cavitation of the vessels during periods with high transpiration demands (Hacke et al. 2001, Cochard et al. 2004a, Brodribb and Holbrook 2005a). In order to maintain gas exchange similar to healthy leaves, leaf water potential has to decrease by way of greater evaporation from the stomata so that adequate volumes of water can reach the leaf. However, infected and non-infected

trees showed a similar course of leaf water potential (Ψ_l) throughout the day, leading to the lower transpiration rate of infected trees. Moreover, when transpiration demands are high at midday, the leaf water potential decreases to its specific minimum (Tyree and Zimmermann 2002), stomata start to close (Yang and Tyree 1993, Brodribb and Holbrook 2003, Klein 2014) and the transpiration rate decreases. In our case, minimum water potential (Ψ_{min}, −1.6 MPa) was not influenced by the presence of fungal hyphae in the water-conducting xylem cells, which is typical for more isohydric species that close their stomata to regulate their leaf water potential at a species-specific minimum (Klein 2014, Martínez-Vilalta et al. 2014). Considering such a value for Ψ_{min} and a gradient of Ψ ~0.5 MPa m^{-1}, the water potential in branches reached values close to −1.0 MPa. Such a water potential could result in a substantial loss of conductivity in small branches of elm trees (Venturas et al. 2013, 2014).

Potential and measured transpiration of branches

Transpiration is directly driven by stomatal conductance and by the leaf-to-air vapour pressure gradient. An increase in both leads to water loss from leaves and generates a water pressure drop in leaves, which is the main driving force for the water transport in xylem. The leaf hydraulic conductance is a major determinant of tree water transport capacity (Sack et al. 2005), which could indirectly affect transpiration when a decrease in hydraulic conductance is translated into a decline in leaf water potential and stomatal closure (Brodribb and Holbrook 2005b). The potential transpiration rate (E_{th}) that we calculated links the xylem capacity for water transport (Lewis and Boose 1995, Tyree and Zimmermann 2002) with its driving force (Tyree 1997) and, as such, could indirectly describe the maximal performance of transpiration for any given condition. It could be expected that E_{th} of healthy ring-porous trees should be slightly higher than the measured transpiration (E_{max}), as the theoretical hydraulic conductivity calculated according to the Hagen–Poiseuille law often overestimates real hydraulic conductivity (Cruiziat et al. 2002, Cochard et al. 2004b). However, in this study, E_{th} of non-infected trees was similar to E_{max} and, in general, E_{th} closely reflected E_{max}. Similar values for theoretical (based on anatomy of petioles) and measured transpiration were also found in laurel forests by Čermák et al. (2002) and for young oak trees (R. Plichta, manuscript in preparation). These results suggest that cross-sectional dimensions of vessels in petioles are not over-dimensioned (Čermák et al. 2002), as they are tightly driven by low cost–efficiency trade-offs (Zimmermann 1978, Sperry 2003, Sperry et al. 2008). The traits E_{th} and E_{max} provided a direct comparison of variables with the same dimensions and units and thus could capture the extent of branch dysfunction and/or potential infestation. In general, infested trees should have a lower E_{max} than E_{th} due to lower hydraulic conductivity. However, the relationship between E_{th} and E did not differ substantially between the two treatments even though E_{th} of infected trees was higher by 20% than E_{max}.

Interestingly, E_{th} was independent of leaf size, although petiole hydraulic conductivity decreased significantly with decreasing leaf size. This independence was caused by the variation in the water potential gradients that occurs between leaves and the base of branches. A comparison of gradients between branches could be complicated by differences in anatomical and hydraulic characteristics, in particular, the hydraulic resistances at junctions (petiole–shoot, shoot–shoot), where the main changes in water potential most often occur (Zimmermann 1978, Tyree and Zimmermann 2002).

Allometric relationships

Leaf traits are often closely associated with plant growth. The leaf area to cross sectional xylem area ratio (HV) is the trait connecting plant hydraulic architecture with carbon allocation (Tyree and Zimmermann 2002, Larcher 2003). However, in this study, HV and HV$_m$ correlated only weakly with other leaf and branch traits. Huber value does not always describe the water-conducting capacity very well, especially in ring-porous species, when it does not take into account the amount of functional xylem (Zimmermann 1978, Tyree and Zimmermann 2002). Therefore, some authors have proposed using the area of sapwood instead of whole xylem area (e.g., Cruiziat et al. 2002). In this study, we did not distinguish the area of sapwood, which in elm trees could be limited to just several of the outermost rings. This could lead to HV variation and a disconnection from other traits.

Leaf mass per area ratio is another fundamental trait that is significantly correlated with a number of other leaf traits (Sack et al. 2003, Sack and Holbrook 2006). Several authors have proposed that LMA is coordinated with a complex of traits that have a bearing on leaf and plant carbon economy and should be more or less independent of transpiration rate (Wright et al. 2004, Sack et al. 2005). However, we found significant, positive relationships between LMA and both leaf area-specific conductivity (k_l) and E_{th}. Moreover, LMA is related to gas exchange variables (Donovan et al. 2011, Ďurkovič et al. 2013). In spite of this, we did not find a relationship between leaf mass-specific conductivity (k_m) and LMA (Nardini et al. 2012). As confirmed by PCA, we found LMA to be correlated more closely with leaf area-specific traits. The reason for this could be that, in contrast to other authors, we focussed on petiole conductivity. The LMA of the examined trees ranged from 86 to 126 g m^{-2} independently of the inoculation treatment. Higher LMA is derived from higher leaf density or thicker leaf lamina (Poorter et al. 2009, Ďurkovič et al. 2012). As we did not find a relationship between LMA and leaf area (A_l), we suppose that the increase we observed in LMA was connected with an increase in leaf thickness (Ďurkovič et al. 2013). Generally, an increase in LMA is associated with higher carbon costs per leaf area, and the

co-occurring increase in k_l and E_{th} in this study could indicate a greater possibility of water supply per leaf area. This is in accordance with increasing LMA in thicker sun leaves, the construction of which consumes more carbon and water (Sack et al. 2003).

Interestingly, branches with abundant and smaller leaves had a total leaf area (A_b) similar to that of branches that bore fewer and larger leaves. The smaller A_l was accompanied by decreasing xylem-specific conductivity in petioles (k_x), as xylem in smaller leaves contained more vessels (increase in vessel elements density, N_n) with lower diameter (decrease in 95th percentile vessel diameter, D_{95}) and thicker cell walls (decrease in vessel lumen area percentage, N_A). Thus, the decrease in A_l resulted in the improvement of leaf tolerance to hydraulic dysfunction (Nardini et al. 2012), which occurred at the expense of higher carbon costs for denser xylem construction. On the other hand, the total carbon cost for such leaf construction could not be higher, as LMA did not increase in smaller leaves.

Conclusion

The results presented here showed that, 3 years following fungal inoculation, the hyphae of *O. novo-ulmi* subsp. *novo-ulmi* × *O. novo-ulmi* subsp. *americana* had no influence on the examined anatomical and morphological traits in 'Dodoens' trees. Both infected and non-infected trees followed the same course of leaf development. Also, physiological measurements did not reveal any substantial decline in tree functionality. On the other hand, the difference in transpiration of branches between infected and non-infected trees highlighted the predisposition of 'Dodoens' trees to xylem dysfunction should they be subjected to new highly aggressive strains of DED in the future. Three years following fungal inoculation, phenotypic expressions for the majority of the examined traits revealed a constitutive nature for their possible role in DED tolerance.

Supplementary data

Supplementary data for this article are available at *Tree Physiology* Online.

Acknowledgments

The authors thank Dr J. Krajňáková for the micropropagated plant material, Drs M. Mamoňová and I. Čaňová for their excellent technical assistance, Mrs E. Ritch-Krč for language revision and two anonymous reviewers for their helpful and constructive comments.

Conflict of interest

None declared.

References

Allen RG, Pereira LS, Raes D, Smith M (1998) Crop evapotranspiration: guidelines for computing crop water requirements. FAO irrigation and drainage paper 56. FAO, Rome.

Bauerle WL, Hinckley TM, Cermak J, Kucera J, Bible K (1999) The canopy water relations of old-growth Douglas-fir trees. Trees 13:211–217.

Binz T, Canevascini G (1996) Xylanases from the Dutch elm disease pathogens *Ophiostoma ulmi* and *Ophiostoma novo-ulmi*. Physiol Mol Plant Pathol 49:159–175.

Brasier CM (2000) Intercontinental spread and continuing evolution of the Dutch elm disease pathogens. In: Dunn CP (ed) The elms: breeding, conservation and disease management. Kluwer Academic Publishers, Boston, pp 61–72.

Bréda N, Huc R, Granier A, Dreyer E (2006) Temperate forest trees and stands under severe drought: a review of ecophysiological responses, adaptation processes and long-term consequences. Ann For Sci 63:625–644.

Brodribb TJ, Holbrook NM (2003) Stomatal closure during leaf dehydration, correlation with other leaf physiological traits. Plant Physiol 132:2166–2173.

Brodribb TJ, Holbrook NM (2005a) Water stress deforms tracheids peripheral to the leaf vein of a tropical conifer. Plant Physiol 137:1139–1146.

Brodribb TJ, Holbrook NM (2005b) Leaf physiology does not predict leaf habit; examples from tropical dry forest. Trees 19:290–295.

Čermák J, Jiménez SM, González-Rodríguez AM, Morales D (2002) Laurel forests in Tenerife, Canary Islands. Trees 16:538–546.

Cochard H, Froux F, Mayr S, Coutand C (2004a) Xylem wall collapse in water-stressed pine needles. Plant Physiol 134:401–408.

Cochard H, Nardini A, Coll L (2004b) Hydraulic architecture of leaf blades: where is the main resistance? Plant Cell Environ 27:1257–1267.

Cruiziat P, Cochard H, Améglio T (2002) Hydraulic architecture of trees: main concepts and results. Ann For Sci 59:723–752.

Dias MC, Oliveira H, Costa A, Santos C (2014) Improving elms performance under drought stress: the pretreatment with abscisic acid. Environ Exp Bot 100:64–73.

Donovan LA, Maherali H, Caruso CM, Huber H, de Kroon H (2011) The evolution of the worldwide leaf economics spectrum. Trends Ecol Evol 26:88–95.

Duchesne L (1993) Mechanisms of resistance: can they help save susceptible elms? In: Sticklen M, Sherald J (eds) Dutch elm disease research: cellular and molecular approaches. Springer, New York, pp 239–254.

Ďurkovič J, Kardošová M, Čaňová I, Lagaňa R, Priwitzer T, Chorvát D Jr, Cicák A, Pichler V (2012) Leaf traits in parental and hybrid species of *Sorbus* (Rosaceae). Am J Bot 99:1489–1500.

Ďurkovič J, Čaňová I, Lagaňa R, Kučerová V, Moravčík M, Priwitzer T, Urban J, Dvořák M, Krajňáková J (2013) Leaf trait dissimilarities between Dutch elm hybrids with a contrasting tolerance to Dutch elm disease. Ann Bot 111:215–227.

Ďurkovič J, Kačík F, Olčák D, Kučerová V, Krajňáková J (2014) Host responses and metabolic profiles of wood components in Dutch elm

hybrids with a contrasting tolerance to Dutch elm disease. Ann Bot 114:47–59.

Ďurkovič J, Kačík F, Olčák D (2015) An evaluation of cellulose degradation affected by Dutch elm disease. Bio-protocol 5:e1535.

Dvořák M, Tomšovský M, Jankovský L, Novotný D (2007) Contribution to identify the causal agents of Dutch elm disease in the Czech Republic. Plant Prot Sci 43:142–145.

Ghelardini L, Santini A (2009) Avoidance by early flushing: a new perspective on Dutch elm disease research. iForest 2:143–153.

Guyot G, Scoffoni C, Sack L (2012) Combined impacts of irradiance and dehydration on leaf hydraulic conductance: insights into vulnerability and stomatal control. Plant Cell Environ 35:857–871.

Hacke UG, Sperry JS, Pockman WT, Davis SD, McCulloh KA (2001) Trends in wood density and structure are linked to prevention of xylem implosion by negative pressure. Oecologia 126:457–461.

Hubbes M (2004) Induced resistance for the control of Dutch elm disease. Investig Agrar Sist Recur For 13:185–196.

Klein T (2014) The variability of stomatal sensitivity to leaf water potential across tree species indicates a continuum between isohydric and anisohydric behaviours. Funct Ecol 28:1313–1320.

Konrad H, Kirisits T, Riegler M, Halmschlager E, Stauffer C (2002) Genetic evidence for natural hybridization between the Dutch elm disease pathogens *Ophiostoma novo-ulmi* ssp. *novo-ulmi* and *O. novo-ulmi* ssp. *americana*. Plant Pathol 51:78–84.

Larcher W (2003) Physiological plant ecology: ecophysiology and stress physiology of functional groups, 4th edn. Springer, Berlin, 513 pp.

Lewis MA, Boose ER (1995) Estimating volume flow rates through xylem conduits. Am J Bot 82:1112–1116.

Limousin JM, Longepierre D, Huc R, Rambal S (2010) Change in hydraulic traits of Mediterranean *Quercus ilex* subjected to long-term throughfall exclusion. Tree Physiol 30:1026–1036.

Martín JA, Solla A, Woodward S, Gil L (2007) Detection of differential changes in lignin composition of elm xylem tissues inoculated with *Ophiostoma novo-ulmi* using Fourier transform-infrared spectroscopy. For Pathol 37:187–191.

Martínez-Vilalta J, Poyatos R, Aguadé D, Retana J, Mencuccini M (2014) A new look at water transport regulation in plants. New Phytol 204:105–115.

Martre P, Durand JL, Cochard H (2000) Changes in axial hydraulic conductivity along elongating leaf blades in relation to xylem maturation in tall fescue. New Phytol 146:235–247.

McDowell N, Barnard H, Bond B et al. (2002) The relationship between tree height and leaf area: sapwood area ratio. Oecologia 132:12–20.

Mencuccini M, Grace J (1995) Climate influences the leaf area/sapwood area ratio in Scots pine. Tree Physiol 15:1–10.

Nardini A, Pedà G, La Rocca N (2012) Trade-offs between leaf hydraulic capacity and drought vulnerability: morpho-anatomical bases, carbon costs and ecological consequences. New Phytol 196:788–798.

Newbanks D, Bosch A, Zimmermann MH (1983) Evidence for xylem dysfunction by embolization in Dutch elm disease. Phytopathology 73:1060–1063.

Nobel PS (2005) Physicochemical and environmental plant physiology, 3rd edn. Elsevier, Burlington, MA, 567 pp.

Otieno DO, Schmidt MWT, Adiku S, Tenhunen J (2005) Physiological and morphological responses to water stress in two *Acacia* species from contrasting habitats. Tree Physiol 25:361–371.

Ouellette GB, Rioux D (1992) Anatomical and physiological aspects of resistance to Dutch elm disease. In: Blanchette RA, Biggs AR (eds) Defense mechanisms of woody plants against fungi. Springer, Berlin, pp 257–307.

Ouellette GB, Rioux D, Simard M, Cherif M (2004) Ultrastructural and cytochemical studies of host and pathogens in some fungal wilt diseases: retro- and introspection towards a better understanding of DED. Invest Agrar Sist Recur For 13:119–145.

Poorter H, Niinemets Ü, Poorter L, Wright IJ, Villar R (2009) Causes and consequences of variation in leaf mass per area (LMA): a meta-analysis. New Phytol 182:565–588.

R Development Core Team (2012) R: a language and environment for statistical computing. R Foundation for Statistical Computing, Vienna, Austria. http://www.R-project.org/ (26 January 2016, date last accessed).

Riceter H (1973) Frictional potential losses and total water potential in plants: a re-evaluation. J Exp Bot 24:983–994.

Sack L, Holbrook NM (2006) Leaf hydraulics. Annu Rev Plant Biol 57:361–381.

Sack L, Cowan PD, Jaikumar N, Holbrook NM (2003) The 'hydrology' of leaves: co-ordination of structure and function in temperate woody species. Plant Cell Environ 26:1343–1356.

Sack L, Tyree MT, Holbrook NM (2005) Leaf hydraulic architecture correlates with regeneration irradiance in tropical rainforest trees. New Phytol 167:403–413.

Smalley EB, Guries RP (1993) Breeding elms for resistance to Dutch elm disease. Annu Rev Phytopathol 31:325–352.

Solla A, Bohnens J, Collin E et al. (2005) Screening European elms for resistance to *Ophiostoma novo-ulmi*. For Sci 51:134–141.

Sperry JS (2003) Evolution of water transport and xylem structure. Int J Plant Sci 164:S115–S127.

Sperry JS, Adler FR, Campbell GS, Comstock JP (1998) Limitation of plant water use by rhizosphere and xylem conductance: results from a model. Plant Cell Environ 21:347–359.

Sperry JS, Meinzer FC, McCulloh KA (2008) Safety and efficiency conflicts in hydraulic architecture: scaling from tissues to trees. Plant Cell Environ 31:632–645.

Svaldi R, Elgersma DM (1982) Further studies on the activity of cell wall degrading enzymes of aggressive and non-aggressive isolates of *Ophiostoma ulmi*. Eur J For Pathol 12:29–36.

Takai S, Richards WC (1978) Cerato-ulmin, a wilting toxin of *Ceratocystis ulmi*: isolation and some properties of cerato-ulmin from the culture of *C. ulmi*. J Phytopathol 91:129–146.

Tyree MT (1997) The Cohesion–Tension theory of sap ascent: current controversies. J Exp Bot 48:1753–1765.

Tyree MT, Zimmermann MH (2002) Xylem structure and the ascent of sap, 2nd edn. Springer, Berlin, 283 pp.

Urban J, Dvořák M (2014) Sap flow-based quantitative indication of progression of Dutch elm disease after inoculation with *Ophiostoma novo-ulmi*. Trees 28:1599–1605.

Van Alfen NK, Turner NC (1975) Influence of a *Ceratocystis ulmi* toxin on water relations of elm (*Ulmus americana*). Plant Physiol 55:312–316.

Venturas M, López R, Gascó A, Gil L (2013) Hydraulic properties of European elms: xylem safety-efficiency tradeoff and species distribution in the Iberian Peninsula. Trees 27:1691–1701.

Venturas M, López R, Martín JA, Gascó A, Gil L (2014) Heritability of *Ulmus minor* resistance to Dutch elm disease and its relationship to vessel size, but not to xylem vulnerability to drought. Plant Pathol 63:500–509.

Woodruff DR, Meinzer FC, Lachenbruch B (2008) Height-related trends in leaf xylem anatomy and shoot hydraulic characteristics in a tall conifer: safety versus efficiency in water transport. New Phytol 180:90–99.

Wright IJ, Reich PB, Westoby M et al. (2004) The worldwide leaf economics spectrum. Nature 428:821–827.

Yang S, Tyree MT (1993) Hydraulic resistance in *Acer saccharum* shoots and its influence on leaf water potential and transpiration. Tree Physiol 12:231–242.

Zimmermann MH (1978) Hydraulic architecture of some diffuse-porous trees. Can J Bot 56:2286–2295.